Experimental and numerical investigation of submicron particle deposition enhancement by patterned surface

IOP Conf. Series: Materials Science and Engineering **609** (2019) 042018 doi:10.1088/1757-899X/609/4/042018

Experimental and numerical investigation of submicron particle deposition enhancement by patterned surface

Haolun Xu[*,1], **Tsz Wai Lai**[1], **Sau Chung Fu**[3], **Chili Wu**[1, 2], **Huihe Qiu**[1], **Christopher Y.H. Chao**[3]

[1] Department of Mechanical and Aerospace Engineering, The Hong Kong University of Science and Technology, Clear Water Bay, Hong Kong
[2] Building Energy Research Center, Fok Ying Tung Research School, HKUST, Hong Kong
[3] Department of Mechanical Engineering, The University of Hong Kong, Pok Fu Lam, Hong Kong
[*] hxubd@connect.ust.hk

Abstract. Exposure to inhaling airborne particles in indoor and outdoor environments is a threat to public health. Indoor air passes through ventilation ducts and continuously circulates with the air outdoors, resulting in a higher concentration of suspended particles in indoor environments when compared to outdoor environments. Thus removing airborne particles in ventilation ducts becomes essential, especially in large buildings. Repeated surface ribs have been reported to greatly enhance the particle collection efficiency while it also causes a significant pressure drop, leading to higher energy consumption. In this study, an overall efficiency ratio is defined, taking into consideration the particle removal rate and the associated pressure drop, to evaluate the overall performance of different surface patterns in a ventilation duct. After the design and optimization processes, the semi-circular patterns are shown to have the best overall efficiency, i.e. a 1137 times increase when compared with having no patterned surface. The deposition velocity on the semi-circular surface found in simulation results were validated with a fully-developed wind tunnel experiment. This study shows that semi-circular surface patterns with a pitch-to-height ratio of 4 are recommended for the overall enhancement in the ventilation duct, especially for capturing submicron particles.

1. Introduction

The side effects of inhalation exposure to airborne particles can be reduced significantly through particle deposition in ventilation ducts. The degree of indoor air quality is assessed by the number of particular matters (PM). The demands to deposit PM, especially in the range of 0.1-1 micrometer in the ventilation duct are strong. Sippola and Nazaroff [1] investigated the particle deposition in ventilation ducts as this is the dominant entry path of outdoor air entering into buildings and circulating with indoor air. Their results indicated that surface roughness is the dominant factor for deposition in insulated ducts. Lai and Nazaroff [2] studied the deposition of 0.9-9 μm particles onto vertical walls with a roughness ranging from 10 to 250 nm. However, the surface roughness still cannot capture a large number of submicron particles because of the lower turbulence kinetic energy among the surface roughness structures. Subsequently Lai et al. [3] compared the particle deposition rate in smooth and ribbed duct air flow by experimental measurements. Their preliminary results indicated that the surface ribs can greatly increase the particle deposition. Lu and Lu [4] numerically studied the particle deposition enhancement of different micro-structured patterns (rectangular, triangular and full-circular ribbed-walls) on a turbulent channel. They defined an efficiency ratio by considering both the effects of particle deposition enhancement and drag force induced by a micro-structured surface. It is found that square ribs are an efficient and effective alternative for efficiency enhancement compared with triangular and circular ribs. But the flow drag is increased to a ratio of 9.8 compared with a plain surface. By reducing the pressure drop, the total efficiency ratio can overwhelm the micro-structured surface discussed above. Therefore,

it is valuable to investigate more micro-structured surface and optimize the dimension for higher deposition enhancement with a reduced drop in pressure.
An overall efficiency including both the particle deposition enhancement and the decrease of fluid drag were defined to compare the performance of different types of surface patterned structures. Our study covered patterned surfaces with rectangular, triangular, semi-circular and open-circular shapes. Computational fluid dynamics (CFD) simulation and experimental validation were used to compare particle deposition enhancement in turbulent flows. In our simulation, *p/e* varied from 3, 4, 5, 6. For each *p/e*, the particle diameter is 0.01, 0.02, 0.1, 0.2, 0.3, 0.5, 1, 1.2, 3, 5, 8 and 20 μm. A recommended patterned surface at a certain *p/e* will be suggested from both the experiment and numerical simulation to increase the energy efficiency of the current ventilation system.

2. Numerical model and methodology

2.1. Turbulent air flow

To model the turbulent airflow interaction with particle motion, a set of Reynolds-averaged Navier-Stokes (*RANS*) equations are selected and solved. In our numerical model, a Reynolds stress model (*RSM*) with velocity fluctuation correction was applied to study the anisotropic flow field [5]. The air dynamic viscosity was 1.789×10^{-5} N·s/m^2, and air density was 1.225 kg/m^3 at a temperature of 288 K. All variables were specified at the inlet and the average inlet air velocity was 5 m/s. The Reynolds number based on average velocity and channel width was 6845. A fully developed turbulent channel flow profile was imposed at the inlet. The inlet velocity is modeled with a 1/7th power law, which is given by

$$U = \frac{8}{7}U_{mean}\left(\frac{y}{h/2}\right)^{1/7} \text{ for } 0 \le y \le \frac{h}{2} \quad (1)$$

$$U = \frac{8}{7}U_{mean}\left(\frac{h-y}{h/2}\right)^{1/7} \text{ for } \frac{h}{2} \le y \le h \quad (2)$$

h is the channel height, U_{mean} is the averaged velocity of the channel, y is the vertical position of the channel. The fully developed turbulence kinetic energy at the inlet is given as,

$$k = \frac{\tau_w}{\rho_g\sqrt{C_\mu}} + \frac{y}{h/2}\left(0.002U_{free}^2 - \frac{\tau_w}{\rho_g\sqrt{C_\mu}}\right) \text{ for } 0 \le y \le \frac{h}{2} \quad (3)$$

$$k = \frac{\tau_w}{\rho_g\sqrt{C_\mu}} + \frac{h-y}{h/2}\left(0.002U_{free}^2 - \frac{\tau_w}{\rho_g\sqrt{C_\mu}}\right) \text{ for } D/2 \le y \le D \quad (4)$$

ρ_g is the density of air, C_μ is an empirical constant specified in the turbulent model (approximately 0.09), U_{free} equals to 8/7 of U_{mean}, τ_w is the wall shear stress.

2.2. Particle trajectory equation

The particles were tracked by Lagrangian particle tracking by considering the effect of lift force, gravitational force, drag force, and Brownian motion. The Lagrangian equations governing the particle motion are written as,

$$m_p\frac{d\overrightarrow{u_p}}{dt} = \vec{F}_{drag} + \vec{F}_{gravitation} + \vec{F}_{Brownian} + \vec{F}_{lift} \quad (5)$$

Particle force terms in Equation 5 are defined in Table 1. In Table 1, the factor C_c is the Cunningham correlation, $\boldsymbol{\lambda}$ is the mean free path, d_p is the particle diameter, Re_p is the Reynolds number of particles, ρ_g is the density of air, υ_g is the kinematic viscosity of air, k_b is the gas constant (1.38×10^{-23}), T is the absolute temperature of air, ρ_p is the density of the particle.

Table 1. Particle trajectory equations

	Submicron particles *(<1μm)*	Micron particles *(>1μm)*
Particle drag force	$\vec{F}_{drag} = \frac{18\mu}{{d_p}^2 \rho_p C_c}$ $C_c = 1 + \frac{2\lambda}{d_p}(1.257 + 0.4e^{-\left(\frac{1.1 d_p}{2\lambda}\right)})$	$F_{drag} = \frac{18\mu}{\rho_p D_p^2}\frac{C_D Re_p}{24}$ $C_D = \frac{24}{Re_p}$ for $Re_p < 1$ $C_D = \frac{24}{Re_p}(1 + 0.15 Re_P^{0.687})$ for $1 < Re_p < 400$
Brownian motion	$F_{Brownian} = \zeta\sqrt{\frac{\pi S_0}{\Delta t}}$, $S_0 = \frac{216\rho_g \upsilon_g k_b T}{\pi^2 \rho_p^2 d_p^5 C_c}$	
Gravitational force	$m_p g$	
Lift force	Saffman's lift force [6]	

3. Numerical results and discussion

The length of the channel is 400 mm and the width of the channel is 20 mm. The height of the surface patterns is 2 mm, which was constant for all the cases. The ratio of rib height to the rib width was 0.5. Figure 1 displayed different types of patterned surface at the *p/e* of 3.

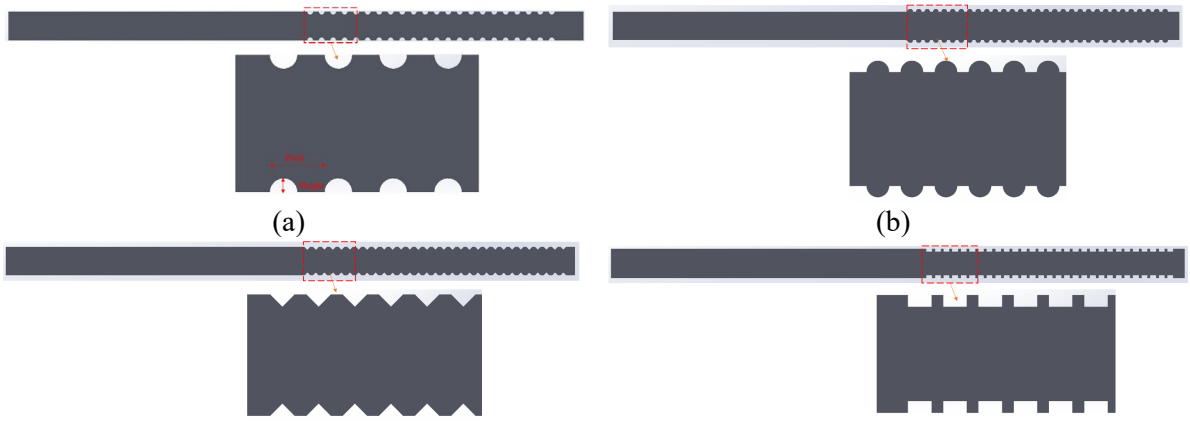

Figure 1. Different types of patterned surfaces for particle deposition: (a) Semi-circular (b) Open circular (c)Triangular ribs (d) Rectangular ribs

An overall performance η is applied in Equation (6) to compare the deposition and fluid performance of different patterns.

$$\eta = \frac{V_{d-rough}/V_{d-smooth}}{F_{d-rough}/F_{d-smooth}} \tag{6}$$

where $V_{d-rough}$ and $V_{d-smooth}$ are the particle deposition velocity of a patterened surface and smooth surface respectively, and $F_{d-rough}$ and $F_{d-smooth}$ are the flow drag for a patterned surface and smooth surface respectively. Figure 2 (a), (b), (c) and (d) illustrate the η for different patterned surfaces under the *p/e* of 3, 4, 5 and 6. It can be seen for different *p/e*, the semi-circular surface pattern overwhelms the other micro-patterns and has the best overall efficiency. The triangular patterned surface has the lowest η. The best η still occurs at the range of submicron-sized particles, while the η decreases with ultrafine and micron-sized particles.

The deposition velocity (V_d) in Equation (6) can be defined as Equation (7),

$$V_d = \frac{J}{n_0} = \frac{particle\ number\ deposited/(Area \cdot t_d)}{particle\ number/m^3} \tag{7}$$

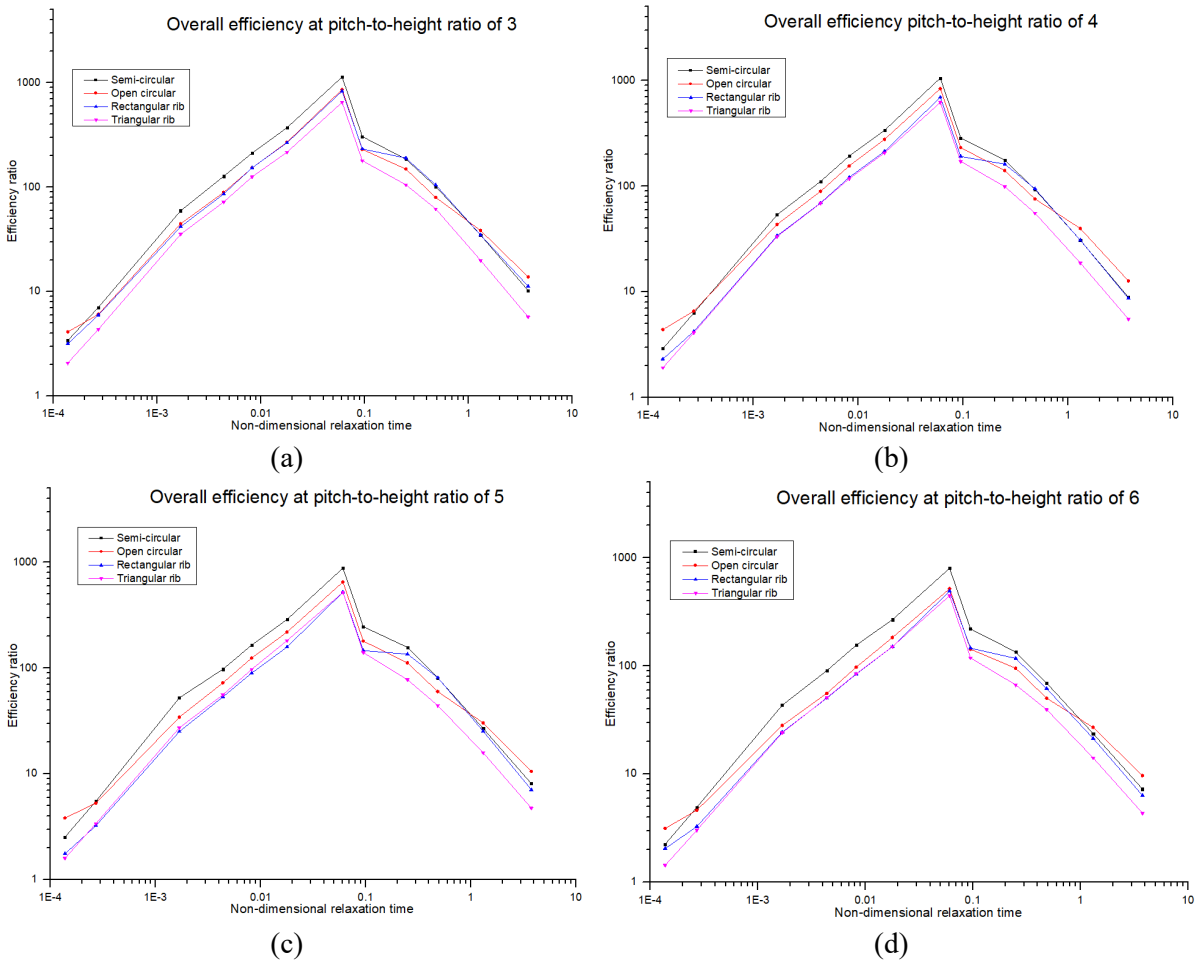

Figure 2. Comparison of overall efficiency for different types of surface patterns under different *p/e*: (a) *p/e*=3 (b) *p/e*=4 (c) *p/e*=5 (d) *p/e*=6

4. Particle deposition experiment and validation

This study included experiments to validate the numerical results. A wind tunnel is set up to provide a fully developed turbulent channel flow [7]. In Figure 3, the wind tunnel consists of a blower, honeycomb, screen and test section. The cross-section of the tunnel is 20 mm in height times 200 mm in width. The test section was located 3 m downstream along the duct, which was 150 times the height of the channel and was sufficient for the flow to develop fully. In the test section, a holder to fit the sample was made and positioned at the centerline of the duct. The entire duct is made of transparent Perspex. The blower is driven by a frequency inverter to induce the airflow in the ducts. In order to compare the experimental results with numerical results, the frequency inverter is maintained at 275 Hz to generate a constant flow velocity of 5.5 m/s. The flow velocity is measured at the middle of the testing section by TSI Model 8386 VelociCalc Plus. In our experiment, TSI 3475 Aerosol Generator generates high-concentration monodisperse aerosols by using di-2-ethyl hexyl sebacate (DEHS) as the aerosol material. The particle size from the aerosol generator has a high concentration of 2.5 μm. A compressed cylinder supplies a constant flow rate of nitrogen at 250 l/h. The TSI 3330 optical particle sizer measures the particle concentration constantly distributed above the patterned surface.

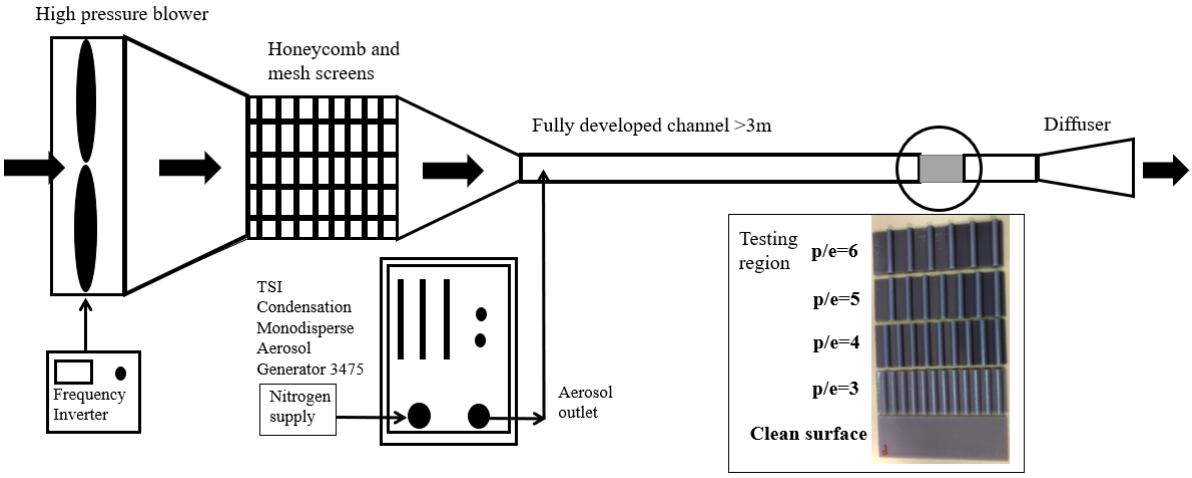

Figure 3. Experimental setup

From numerical simulation results (Section 3), the best overall efficiency among these optimized shapes is the semi-circular patterned surface. The experimental deposition velocity was tested and compared between a clean surface and the semi-circular shape at *p/e*=3, *p/e*=4, *p/e*=5 and *p/e*=6. In Figure 3, the height of the semi-circular surface is 2 mm, which is consistent with the numerical geometry. Figure 4 displays the results of a particle deposition experiment with a clean surface and semi-circular patterned surface at the *p/e* of 4. The photos are taken by a Nikon eclipse Ni-E microscope. Figure 4(a) and (b) are views on the clean surface before and after deposition. Figure 4(c) and (d) are views displayed on the bottom surface between semi-circular structure before and after deposition. Each view in Figure 4 (a)-(d) represents a rectangular range of 790 μm×790 μm. The particle deposition on the semi-circular surface is more obvious than the particle deposition on the clean surface.

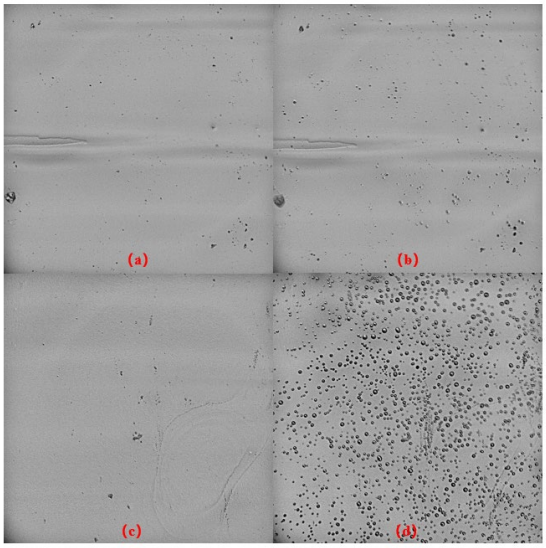

Figure 4. Particle deposition experiment: Clean surface (a) before and (b) after deposition; Semi-circular surface at *p/e*=4 (c) before and (d) after deposition

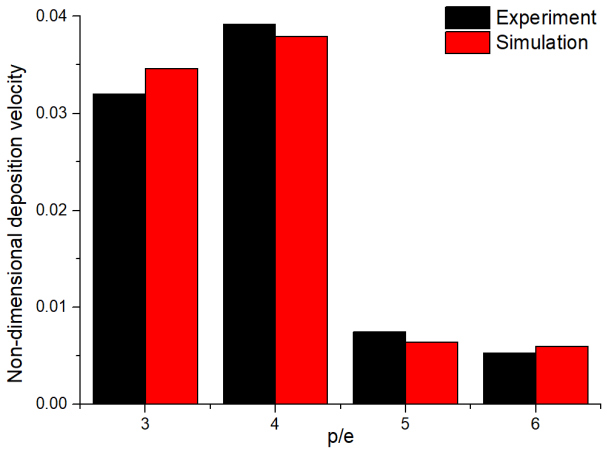

Figure 5. Comparison of particle deposition velocity between experiment (black) and numerical simulation (red)

A deposition velocity will be calculated based on the particle deposition number and undisturbed particle concentration (measured by GRIMM particle sizer). After the figures were observed under the

microscope, the deposited particles were contrasted against the background. The contact area of each particle was identified by using ImageJ software.

$$A_{s-l} = \pi V_{cap}^{2/3} \left[\frac{\pi}{3}(2 - 3cos\alpha + cos^3\alpha)\right]^{-2/3} sin^2\alpha \quad (8)$$

Based on the area of planar surface under the microscope visualization, the volume of aerosol deposited in each picture can be determined by Equation (8). The particle deposition number N_d can be obtained by using the volume of each droplet divided by the volume of each monodispersed aerosol. The deposition duration t_d is 10 minutes. The comparison of particle deposition velocity for different *p/e* of a semi-circular shape between experiment (black) and numerical simulation (red) is displayed in Figure 5. The largest discrepancy between the experiment and numerical simulation at the *p/e* of 4 is 26.5%. The highest deposition velocity happens at *p/e*=4 for the semi-circular patterned surface.

5. Conclusions

Particle deposition enhancement by various patterns of surface rib (rectangular, triangular, semi-circular and open-circular) are presented in this work by using the Reynolds stress turbulent model and Lagrangian particle tracking. The semi-circular pattern has the highest overall efficiency when compared with other patterned surfaces for all *p/e* conditions. The numerical simulation results were then compared and validated with experimental deposition velocity. At *p/e*=4, the experiment and numerical simulation both indicate the highest deposition velocity for the semi-circular patterned surface. Thus the semi-circular patterned surface is recommended to be used in ventilation ducts to enhance the particle deposition as well as increase the energy efficiency of large buildings.

Acknowledgment

This project was supported by a HKSAR General Research Fund (GRF) project (no.16207817, no. 16200315 and no. 16206918).

References

[1] Sippola M R and Nazaroff W W 2004 Experiments measuring particle deposition from fully developed turbulent flow in ventilation ducts *Aerosol Science and technology* **38** 914-25
[2] Lai A and Nazaroff W 2005 Supermicron particle deposition from turbulent chamber flow onto smooth and rough vertical surfaces *Atmospheric Environment* **39** 4893-900
[3] Lai A C, Byrne M A and Goddard A J 2001 Aerosol deposition in turbulent channel flow on a regular array of three-dimensional roughness elements *Journal of Aerosol Science* **32** 121-37
[4] Lu H and Lu L 2015 A numerical study of particle deposition in ribbed duct flow with different rib shapes *Building and Environment* **94** 43-53
[5] Xu H, Fu S C, Leung W T, Lai T W and Chao C Y H 2019 Enhancement of submicron particle deposition on a semi-circular surface in turbulent flow *Indoor and Built Environment* **0** 1-16
[6] Saffman P 1965 The lift on a small sphere in a slow shear flow *Journal of fluid mechanics* **22** 385-400
[7] Fu S, Leung W and Chao C Y 2014 Detachment of droplets in a fully developed turbulent channel flow *Aerosol Science and Technology* **48** 916-23